

# Fine-structure electron-impact excitation of Ne<sup>+</sup> and Ne<sup>2+</sup> for low temperature astrophysical plasmas

Qianxia Wang<sup>1,2</sup>, S. D. Loch<sup>1\*</sup>, Y. Li<sup>1</sup>, M. S. Pindzola<sup>1</sup>, R. S. Cumbee<sup>3,4</sup>,  
P. C. Stancil<sup>3</sup>, B. M. McLaughlin<sup>5</sup> and C. P. Ballance<sup>5†</sup>

<sup>1</sup>*Department of Physics, Auburn University, Auburn, AL 36849, USA*

<sup>2</sup>*Department of Physics and Astronomy, Rice University, Houston, TX 77005, USA*

<sup>3</sup>*Department of Physics and Astronomy and Center for Simulational Physics, University of Georgia, Athens, GA 30602, USA*

<sup>4</sup>*NASA Goddard Space Flight Center, Greenbelt, MD 20771, USA*

<sup>5</sup>*Centre for Theoretical Atomic and Molecular Physics (CTAMOP), School of Mathematics and Physics, Queen's University Belfast, Belfast BT7 1NN, Northern Ireland, UK*

Accepted March 2, 2017. Received July 11, 2016; in original form

## ABSTRACT

Collision strengths for electron-impact of the fine-structure levels within the ground term of Ne<sup>+</sup> and Ne<sup>2+</sup> are calculated using the Breit-Pauli and DARC *R*-matrix methods. Maxwellian-averaged effective collision strengths are presented for each ion. The application of the current calculations is to very low temperature astrophysical plasmas, down to 10 K, thus we examine the sensitivity of the effective collision strengths to the resonance positions and underlying atomic structure. The use of the various theoretical methods allows us to place estimated uncertainties on the recommended effective collision strengths. Good agreement is found with previous *R*-matrix calculations at higher temperatures.

**Key words:** atomic data – atomic process

## 1 INTRODUCTION

Electron-impact fine-structure excitation of low charged ions is an important cooling mechanism in most interstellar environments, especially in regions with significant ionization fraction where electron-impact excitation is a strong populating mechanism for the excited states. The lines from these fine-structure transitions can be observed from the infrared (IR) to the submillimeter (submm) by a range of telescopes (e.g., the *Spitzer Space Telescope*, the Stratospheric Observatory for Infrared Astronomy (SOFIA), the *Herschel Space Observatory*, the Atacama Large Millimeter Array (ALMA), etc.). Furthermore, fine-structure excitation due to electron-impact is an important diagnostic tool for the density, pressure, temperature, and/or ambient radiation field, if sufficiently accurate rate coefficients can be obtained. Electron impact fine-structure excitation has been studied fairly extensively for many ions over the past few decades (Pradhan 1974; Butler & Mendoza 1984; Johnson & Kingston 1997; Saraph 1978; Saraph & Tully 1994; Griffin et al. 2001; Colgan et al. 2003; Berrington et al. 2005; Witthoef et al. 2007; Munoz Burgos et al. 2009; Ludlow et al. 2011; Malespin et al.

2011; McLaughlin et al. 2011; Wu et al. 2012; Abdel-Naby et al. 2013, 2015) with *R*-matrix data being used in most modeling databases. However, almost all of these studies have primarily focused on high energies/high temperatures relevant to collisionally-ionized plasmas, thus much of the low temperature data being used has been extrapolated from the available *R*-matrix data. Also, no detailed study has been taken on the uncertainty of the low temperature rate coefficients. Thus, the aim of this paper is to produce a set of recommended fine structure rate coefficients for the ground term of Ne<sup>+</sup> and Ne<sup>2+</sup>, along with an estimated set of uncertainties.

For plasmas of importance in this paper, we require rate coefficients down to approximately 10 K, appreciating that achieving the accuracy in the underlying cross section at this temperature is difficult. Therefore it is important for astrophysical models that collisional calculations are performed of sufficient accuracy at lower energies for the low temperature rate coefficients. This will extend the available data down to lower temperatures than exist currently in databases and will also improve the accuracy of the low temperature rate coefficients.

The fine-structure line emissions from Ne II and Ne III, populated via electron-impact excitation, are observed in the IR and are known to be very important for probing

\* lochstu@auburn.edu

† c.ballance@qub.ac.uk

H II regions. Previous work (Glassgold et al. 2007; Meijerink et al. 2008) proposed that Ne II and Ne III fine-structure lines could serve as a diagnostic of the source of an evaporative flow, as well as of signatures of X-ray irradiation, the so-called X-ray dominated regions (XDRs). This is because hard X-rays have sufficient energy to generate multiple ionization states of neon which can then be collisionally excited. *R*-matrix calculations have been available for these and neighbouring ion stages of Ne. Specifically, collision strengths for the  $1s^2 2s^2 2p^5$  ( $^2P_{3/2}^0$ ) - ( $^2P_{1/2}^0$ ) transition of Ne<sup>+</sup> have been calculated using a *R*-matrix method via the JAJOM approach (Saraph 1978; Johnson & Kingston 1997; Saraph & Tully 1994), that transforms *LS*-coupled *K*-matrices into level-level cross sections. The collision strengths of the transitions among levels of the lowest configurations for Ne<sup>2+</sup> were evaluated by Pradhan (1974) and Butler & Mendoza (1984) using the IMPACT close-coupling code. McLaughlin et al. (McLaughlin & Bell 2000; McLaughlin et al. 2002, 2011) extended this approach to a large configuration-interaction representation of the target, supplemented by a few extra pseudo-orbitals to improve the target description further.

Here, we have re-investigated these two Ne ions for several reasons. Previous work has focused primarily on higher electron-impact energies than considered here with only a few of their Maxwellian averaged effective collision strengths going below 800 K. Thus, we investigate the sensitivity of the very low temperature rate coefficients to changes in the atomic structure, threshold energies, and resonance positions. This leads naturally to the second focus of the paper, which is the exploration of uncertainty in the rate coefficients at very low temperatures. To this end, two different theoretical level-resolved *R*-matrix approaches have been applied: the Breit-Pauli (BP) approximation (Berrington 1987) and the fully relativistic Dirac method (Norrington & Grant 1981; Dyall et al. 1989; Grant 2007). Ostensibly, if the underlying electronic structure adopted in each approach was exactly the same there would be little expectation of differences in the collision strengths. However, with the use of different atomic structure codes and the choices made in their use, this invariably leads to small differences in transition probabilities (Einstein A coefficients) and subsequently, dynamical quantities such as collision strengths.

Due to the low temperature focus of this paper, we are interested in the sensitivity of the effective collision strengths to the threshold energy position, the target wave-functions, resonance positions, and anything that can affect the background cross section. We appreciate that the height and position of a single resonance can dramatically affect the results at these temperatures. We shall explore the variation in results to threshold energy and resonance positions by calculating collision strengths where the target energies have been shifted (or not) to NIST energies (Kramida et al. 2015). Furthermore, we explore the sensitivity of the target wave-function via different target expansions within the BP *R*-matrix and DARC *R*-matrix methods. After investigating the differences between all calculated effective collision strengths for the same transition, a recommended dataset is determined for each ion.

We focus on excitation at low temperatures (10 -2000 K) in this paper. So for Ne<sup>+</sup>, only rates for the transition

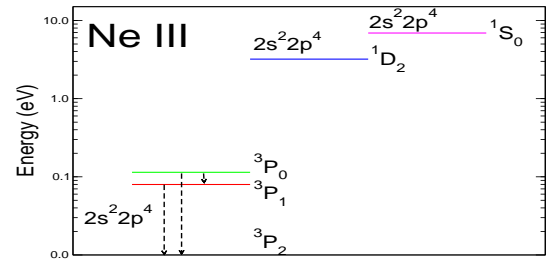


**Figure 1.** Energy diagram for Ne III. Three fine-structure transitions are shown:  $2s^2 2p^4$  ( $^3P_1$ ) - ( $^3P_2$ ),  $2s^2 2p^4$  ( $^3P_0$ ) - ( $^3P_1$ ), and  $2s^2 2p^4$  ( $^3P_0$ ) - ( $^3P_2$ ).

between the two lowest levels  $1s^2 2s^2 2p^5$  ( $^2P_{3/2}^0$ ) - ( $^2P_{1/2}^0$ ) are presented. Also, the transitions between the three lowest fine-structure levels of Ne<sup>2+</sup> (see energy diagram in Figure 1) are investigated here.

The rest of this article is organized as follows. In Sec. 2, we describe the theoretical methods used in this paper. Sec. 3 presents the details of the calculations. The calculated results, target energies, Einstein A coefficients, collision strengths and effective collision strengths for Ne<sup>+</sup> and Ne<sup>2+</sup> will be discussed in Sec. 4. Sec. 5 provides a summary of the results.

## 2 THEORY

Level-resolved electron-impact excitation cross-section calculations using *R*-matrix theory, employs a similar formalism either in semi-relativistic (BP) or relativistic (DARC) implementations. Ne<sup>+</sup> and Ne<sup>2+</sup> are not highly charged, therefore both semi-relativistic and fully relativistic methods are equally applicable. The main differences arise from the choices made in the determination of the target orbitals for use in dynamical calculations. The atomic structure code AUTOSTRUCTURE (Badnell 1986) generates non-relativistic orbitals whereas the General Relativistic Atomic Structure Package (GRASP; Dyall et al. (1989); Grant (2007)) formulates and diagonalises a Dirac-Coulomb Hamiltonian to produce the relativistic orbitals. The former is used in the BP/ICFT (Berrington et al. 1995; Griffin & Badnell 1998) *R*-matrix collisional calculations and the latter in the Dirac Atomic *R*-matrix Code (DARC) (Chang 1975; Norrington & Grant 1981; Grant 2007) calculations to obtain level-to-level electron impact excitation (EIE) cross sections.

The BP  $R$ -matrix method is a set of parallel codes developed from modified serial versions of the RMATRIX I codes (Berrington et al. 1995). Both the BP and ICFT models recouple underlying  $LS$  coupling calculations, the former transforms several  $LS$ -resolved Hamiltonians into a  $jK$ -coupled Hamiltonian as opposed to the ICFT approach that transforms unphysical  $LS$ -resolved  $K$ -matrices into level-resolved collision strengths. In general there has been very good agreement between the ICFT and BP  $R$ -matrix methods (Griffin & Badnell 1998; Munoz Burgos et al. 2009; McLaughlin et al. 2011).

The implementation of various flavours of  $R$ -matrix theory are used in this study. The review book of Burke (Burke 2011) provides an excellent overview of non-relativistic ( $LS$  coupling), semi-relativistic (BP/ICFT) and relativistic (DARC) electron-impact excitation. The comparison of BP and ICFT results benefits from the use of a completely consistent atomic structure calculation. Thus, the comparison with the multiconfiguration Dirac-Fock (MCDF) structure results from GRASP and the resulting DARC collision strengths, provides a means to investigate effects due to changes in the target structure. In all cases every effort has been made to optimize the orbitals on the fine-structure levels of the ground term. The DARC calculation employs relativistic orbitals from the initial atomic structure calculations throughout the remainder of the computation. It should be restated that low temperature astrophysical constraints on both our Ne systems means we are pursuing only transitions between the fine-structure levels of the ground term, and that any excited states are included for the main purpose of improving the energy levels of those low-lying states through configuration interaction. Given that the energy separation between the ground state  $n = 2$  and the excited  $n = 3$  levels for either  $\text{Ne}^+$  or  $\text{Ne}^{2+}$  exceeds 2 Ryd., it is unlikely that Rydberg states attached to the  $n = 3$  levels would perturb our  $n = 2$  results.

### 3 CALCULATION DETAILS

#### 3.1 Target state calculation

Given the low temperature focus of this paper, only small scale calculations are required for the fine-structure transitions within the ground term. Furthermore, we explore the variation of our results in relation to various configuration-interaction (CI) expansions. Thus, we consider both a small and larger CI expansion for  $\text{Ne}^+$  and  $\text{Ne}^{2+}$ , with the configurations described in Table 1. The models are referred to as BP  $n = 2$ , DARC  $n = 2$ , BP  $n = 3$ , and DARC  $n = 3$ .

Orbitals are optimized automatically using the GRASP code (Dyall et al. 1989; Grant 2007), which are then used in subsequent scattering calculation within the Dirac  $R$ -matrix method. We focus on low energies, the orbitals of interest belong then to the first several terms. Scattering calculations for the DARC  $n = 3$  model use orbitals obtained from GRASP from the DARC  $n = 2$  model, which are held fixed. This improves the energies and A-values of the levels in the ground term. We note if all orbitals are optimized simultaneously in a GRASP  $n=3$  calculation this leads to much larger differences with NIST values. Thus, our GRASP  $n=2$  and  $n=3$  calculations for both ions are optimized for the

fine-structure levels of interest to this work. In the GRASP calculations for each ion we used the option of extended average level (EAL) to optimize the energies.

For the BP scattering models, we optimize the target input orbitals using AUTOSTRUCTURE (Badnell 1986) with different sets of parameters. We developed a code to vary the orbital scaling parameters used in AUTOSTRUCTURE, comparing the resulting energies and A-values with NIST values until a minimum was found in the differences (for the transitions of interest) with the NIST tabulated values (Kramida et al. 2015). The optimized orbital scaling parameters are as follows;  $\lambda_{1s}=0.8$ ,  $\lambda_{2s}=1.2$ , and  $\lambda_{2p}=1.08$  for BP  $n = 2$  calculations of Ne III. For the BP  $n = 3$  calculations of Ne III:  $\lambda_{1s}=0.8$ ,  $\lambda_{2s}=1.2$ ,  $\lambda_{2p}=1.08$ ,  $\lambda_{3s}=0.8$ ,  $\lambda_{3p}=1.2$ , and  $\lambda_{3d}=0.8$ .

Similarly, we use the same procedure to generate parameters for the target orbitals for Ne II BP  $n = 2$  and  $n = 3$  collision models. However, in this case we find that the resulting effective collision strengths do not change much compared with the unoptimized structure results, we therefore adopted the unoptimized parameters for the target orbitals in our BP collision calculations for  $\text{Ne}^+$  in this paper. It should be noted that these BP results for Ne II will not be used for our recommended data, and instead will be used only in estimating the uncertainty on our final data.

#### 3.2 Scattering calculation

Details specific to the current  $R$ -matrix calculations are summarized in Table 2, where we have included all the relevant parameters used in the different calculations. The radius of the  $R$ -matrix sphere for the different collision calculations is selected automatically during the  $R$ -matrix calculations. The number of continuum basis orbitals for each angular momentum and partial waves are chosen to converge the results for the low temperature calculations. The energy mesh is selected to ensure resonances were fully resolved, particularly for the lowest temperatures and the subsequent effective collision strengths. The energy ranges calculated for the collision strengths are determined by the effective collision strengths temperature range of interest. It should also be noted that all of the energy levels in the target structure calculations were included in the scattering calculations.

#### 3.3 Effective collision strength calculation

The effective collision strength (Seaton 1953; Eissner et al. 1969) can be calculated from the collision strengths via:

$$\Upsilon_{ij} = \int_0^\infty \Omega_{ij} \exp\left(\frac{-\epsilon_j}{kT_e}\right) d\left(\frac{\epsilon_j}{kT_e}\right), \quad (1)$$

where  $\Omega_{ij}$  is the collision strength for the transition from level  $i$  to  $j$ ,  $\epsilon_j$  is the energy of the scattered electron,  $T_e$  the electron temperature, and  $k$  Boltzmann's constant.

The Maxwellian excitation rate coefficient,  $q_{ij}$ , is used widely in astrophysical modeling codes. The relationship between  $q_{ij}$  and  $\Upsilon_{ij}$  is

$$q_{ij} = 2\sqrt{\pi} \alpha c a_0^2 \left(\frac{I_H}{kT_e}\right)^{1/2} \frac{1}{\omega_i} e^{-\frac{\Delta E_{ij}}{kT_e}} \Upsilon_{ij}, \quad (2)$$

where  $\alpha$  is the fine-structure constant,  $c$  the speed of light,

Ne <sup>+</sup> DARC/BP $n = 2$	Ne <sup>+</sup> DARC/BP $n = 3$	Ne <sup>2+</sup> DARC/BP $n = 2$	Ne <sup>2+</sup> DARC/BP $n = 3$
1s <sup>2</sup> 2s <sup>2</sup> 2p <sup>5</sup>	1s <sup>2</sup> 2s <sup>2</sup> 2p <sup>5</sup>	1s <sup>2</sup> 2s <sup>2</sup> 2p <sup>4</sup>	1s <sup>2</sup> 2s <sup>2</sup> 2p <sup>4</sup>
1s <sup>2</sup> 2s2p <sup>6</sup>	1s <sup>2</sup> 2s2p <sup>6</sup>	1s <sup>2</sup> 2p <sup>6</sup>	1s <sup>2</sup> 2p <sup>6</sup>
	1s <sup>2</sup> 2s2p <sup>5</sup> 3l	1s <sup>2</sup> 2s2p <sup>5</sup>	1s <sup>2</sup> 2s2p <sup>5</sup>
	1s <sup>2</sup> 2s <sup>2</sup> 2p <sup>4</sup> 3l		1s <sup>2</sup> 2s2p <sup>4</sup> 3l
			1s <sup>2</sup> 2s <sup>2</sup> 2p <sup>3</sup> 3l
			1s <sup>2</sup> 2p <sup>5</sup> 3l

**Table 1.** Target expansions for Ne<sup>+</sup> and Ne<sup>2+</sup>.**Table 2.** Scattering calculation parameters used in our work on Ne II and Ne III ions for different target expansions.

	Ne II $n = 2$	Ne II $n = 3$	Ne III $n = 2$	Ne III $n = 3$
	DARC, BP	DARC, BP	DARC, BP	DARC, BP
Radius of $R$ -matrix sphere (a.u.)	5.40, 5.87	19.83, 21.60	4.89, 5.24	13.28, 14.35
Continuum basis orbitals for each angular momentum	20	20	20	20
Partial waves $J$	0 – 20	0 – 20	0 – 20	0 – 20
Energy mesh (Ryd.)	$2.5 \times 10^{-6}$	$2.5 \times 10^{-6}$	$3.125 \times 10^{-6}$	$3.125 \times 10^{-6}$
Energy range (Ryd.)	0.007 – 0.107	0.007 – 0.107	0.0058 – 0.1658	0.0058 – 0.1658
Temperature range (K)	10 – 2000	10 – 2000	10 – 2000	10 – 2000

$a_0$  the Bohr radius,  $I_H$  the hydrogen ionization potential,  $\Delta E_{ij}$  the energy difference in the fine-structure levels, and  $\omega_i$  the degeneracy in the lower level. Compared with  $q_{ij}(T_e)$ ,  $\Upsilon_{ij}(T_e)$  is a smoother function and can be more accurately interpolated.

## 4 RESULTS AND DISCUSSION

Astrophysical plasma modellers who study IR/submm observations of low temperature plasmas, such as the interstellar medium, require atomic rate coefficients down to temperatures as low as 10 K. This will place very stringent tests on the accuracy of the atomic structure and collisional calculations. The excitation rate coefficients will be very sensitive to small changes in the atomic structure. As a result, the structure will impact the rate coefficients through changes in the threshold energy, resonance strengths and positions, and changes in the background cross section. For this reason, we have performed a range of calculations using different methods (BP  $n = 2$ , DARC  $n = 2$ , BP  $n = 3$ , and DARC  $n = 3$ ). These will be used to explore the variation of the effective collision strengths, particularly at low temperatures. The purpose of including the  $n = 3$  configurations is to improve the energies and transition probabilities for the levels within the ground term.

### 4.1 Bound-state energies and radiative rates for Ne<sup>+</sup> and Ne<sup>2+</sup>

Our recommended dataset shall be the model that minimizes the difference between the calculations and NIST A-values and level energies (Kramida et al. 2015). The results are shown in Tables 3 and 4. The percent error ( $\delta\%$ ) shown is calculated by  $\frac{x-x_{NIST}}{x_{NIST}} \times 100\%$  with the NIST data providing the accepted values.

AUTOSTRUCTURE (Badnell 1986) and GRASP (Dyall et al. 1989; Grant 2007) are two different atomic structure codes used to generate target energies and orbitals for the BP and DARC R-matrix methods respectively. They give rise to 3 and 108 levels for Ne<sup>+</sup>, and 10 and 226 levels

for Ne<sup>2+</sup> for  $n = 2$  and  $n = 3$  target expansions. The energies for the levels within the ground term are presented in Table 3 and the associated A-values in Table 4. In general, the percentage errors show that the agreement between theoretical and NIST values is reasonable. For Ne<sup>+</sup>, the average percentage error for the BP  $n = 2$ , BP  $n = 3$ , DARC  $n = 2$ , and DARC  $n = 3$  target expansions are 1.41%, 0.96%, 3.6% and 5.65%, respectively. For Ne<sup>2+</sup>, the corresponding average percent errors for target energies are 2.57%, 3.29%, 3.72% and 4.45%.

Table 4 presents the comparison of Einstein A coefficients of the magnetic-dipole (M1) for both the Ne<sup>+</sup> and Ne<sup>2+</sup> transitions. Due to the reasonable agreement for all the calculations with NIST energies, we use the A-values as our main selection criteria in recommending a final dataset for Ne<sup>+</sup> and Ne<sup>2+</sup>. In both cases, the GRASP code produces closer agreement with NIST A values, compared with AUTOSTRUCTURE. The accuracy of the Einstein A coefficient depends on both the precision of the target energies and the reliability of the target wave-functions. The A values produced by GRASP  $n=2$  and  $n=3$  are close, because they use the same orbitals. Overall the  $n=2$  GRASP calculation has slightly better agreement with NIST A values and energies than the GRASP  $n=3$  calculation, thus our recommended dataset for both ions is the DARC  $n = 2$  calculation. The other calculations can be used to gauge the variation between the different calculations, and will be used to produce an uncertainty estimate on our recommended data.

### 4.2 Collision strengths and effective collision strengths for Ne<sup>+</sup> and Ne<sup>2+</sup>

To our knowledge, there are no experimental results for the collision strengths for transitions within the ground complex for either of these ion stages. Our goal is to determine the variation in effective collision strengths between our best models as we progress to the very low temperatures required by the astrophysical applications. As stated above, the DIRAC  $n=2$  effective collision strengths will be our recommended data, with the some of the other calcula-

**Table 3.** Fine-structure energy levels for Ne II and Ne III (in Ry) compared to the NIST values (Kramida et al. 2015). The configurations and terms listed in the first two columns label different levels. Column 3 gives the corresponding energies from the tabulated NIST values. The percent error after each theoretical energy indicates the deviation from the NIST value. The last line for each ion in the table is the average error  $\delta\%$  of each theoretical calculation.

Configuration	Term ( $2s+1L_J$ )	NIST	BP $n = 2$	$\delta\%$	BP $n = 3$	$\delta\%$	DARC $n = 2$	$\delta\%$	DARC $n = 3$	$\delta\%$
Ne II $2s^22p^5$	$^2P^0_{3/2}$	0.0000	0.0000	0	0.0000	0	0.0000	0	0.0000	0
	$^2P^0_{1/2}$	0.0071	0.0069	2.82	0.0070	1.91	0.0076	7.2	0.0079	11.3
	Avg. $\delta\%$			1.41		0.96		3.6		5.65
Ne III $2s^22p^4$	$^3P_2$	0.0000	0.0000	0	0.0000	0	0.0000	0	0.0000	0
	$^3P_1$	0.0059	0.0057	3.39	0.0057	3.39	0.0060	1.59	0.0061	3.39
	$^3P_0$	0.0084	0.0084	0	0.0083	1.19	0.0088	4.33	0.0090	7.14
	$^1D_2$	0.2355	0.2513	6.70	0.2557	8.58	0.2521	7.05	0.2470	4.88
	$^1S_0$	0.5081	0.4942	2.76	0.4914	3.29	0.4795	5.62	0.4734	6.83
Avg. $\delta\%$			2.57		3.29		3.72		4.45	

**Table 4.** Einstein A coefficients (in  $s^{-1}$ ) for magnetic-dipole-transitions (M1), within the same configuration, for the Ne II and Ne III ions compared to the NIST values (Kramida et al. 2015). Columns are as in Table 3.

Ion	Transition	NIST	BP $n = 2$	$\delta\%$	BP $n = 3$	$\delta\%$	DARC $n = 2$	$\delta\%$	DARC $n = 3$	$\delta\%$
Ne II	$2s^22p^5 (^2P^0_{3/2}) - (^2P^0_{1/2})$	8.59E-3	7.84E-3	8.68	8.07E-3	6.1	8.16E-3	5.01	8.14E-3	5.24
Ne III	$2s^22p^4 (^3P_2) - (^3P_1)$	5.84E-3	5.47E-3	6.34	5.42E-3	7.19	5.86E-3	0.42	5.81E-3	0.51
	$2s^22p^4 (^3P_1) - (^3P_0)$	1.10E-3	1.38E-3	25.45	1.36E-3	23.64	1.15E-3	4.95	1.14E-3	3.64
Avg. $\delta\%$				15.90		15.42		2.69		2.08

tions being used to provide an uncertainty estimate. We have considered two different approaches to calculating meaningful representative uncertainties in our work.

In the first approach we calculate a percentage uncertainty on the effective collision strengths simply using the standard deviation of our three most accurate models as determined from the accuracy of the energy levels and the associated A-values, given by

$$\% \Delta = \frac{\sigma(\bar{x}_{best})}{x_i} \times 100\% \quad (3)$$

where  $\sigma(\bar{x}_{best})$  is the standard deviation. Secondly, we obtain a percentage difference comparing results from our semi-relativistic and fully-relativistic  $R$ -matrix methods employing exactly the same set of non-relativistic target configurations. In this case, the percentage difference is calculated by the formula  $\frac{x_1 - x_2}{(x_1 + x_2)/2} \times 100\%$ .

Figures 2 – 5 illustrate the collision strengths and effective collision strengths for the fine-structure transitions of both  $Ne^+$  and  $Ne^{2+}$ , using the different  $R$ -matrix methods. In the evaluation of these effective collision strengths we use only our best calculations (i.e. optimized  $\lambda$ s where possible and with threshold energies shifted to NIST values). It is, however, interesting to investigate the effect of shifting to NIST energies on the effective collision strengths, thus figures 6 – 8 explore the effects of shifting the target threshold energies to NIST values using the BP  $n=3$  calculation for  $Ne^{2+}$ .

Sampling a range of calculations allows us to more objectively explore the variation of collision strength in regards to the size of the different CI expansions. As stated earlier, the sizeable energy separation between the  $n = 2$  and  $n = 3$  levels precludes the possibility of interloping resonances attached to the  $n = 3$  levels perturbing the cross sections from transitions amongst the  $n = 2$  levels. The influence of resonance contributions to effective collision strengths is only expected for the case of  $Ne^{2+}$  due to the  $2p^4$  subshell sup-

porting 3 levels within the ground term, whereas the resonances attached to the upper  $J = \frac{1}{2}$  levels of  $Ne^+(2p^5)$  lie in the elastic cross section of the  $Ne^+$  ground state.

Figure 2 shows collision strengths (top) and effective collision strengths (bottom) for the  $Ne^+ 2s^22p^5(^2P^0_{3/2}) - (^2P^0_{1/2})$  transition. The largest collision strengths are from the BP  $n = 2$  calculation, the next lower one is from the DARC  $n = 2$  calculation, then from DARC  $n = 3$  and BP  $n = 3$ . The DARC  $n = 2$  calculation is our recommended data set based upon A-value comparisons with the NIST database values (Kramida et al. 2015). Furthermore, in the absence of experiment, the MCDF approach would be our recommended theoretical model. Subsequent effective collision strengths were generated from the respective collision strengths of each calculation. We note that beyond the current work, a previous large-scale BP  $R$ -matrix calculation for  $Ne^+$  has been carried out by Griffin et al. (2001). However, the focus of that work was to provide a large comprehensive data set across a wide range of temperatures, but not at the very low temperatures required by our study. At 1000 and 2000 K, the DARC  $n = 2$  effective collision strengths are in reasonable agreement with this previous work. Our effective collision strengths are 0.302 at 1000 K and 0.304 at 2000 K, compared with 0.266 and 0.286 from (Griffin et al. 2001), as shown in Fig. 2, giving differences of 12.7% and 6.1%, respectively. Thus, this supports our independent conclusion that our DARC  $n = 2$  effective collision strengths should be the recommended dataset at even lower temperatures. The recommended effective collision strengths are given in Table 5. These results can also be obtained in the formats of the Leiden Atomic and Molecular Database (LAMDA, Schöier et al. (2005)) and Stout Lykins et al. (2015).

Employing the average percentage uncertainty given by Equation (3), the  $\bar{x}_{best}$  values used to calculate the uncertainty are the BP  $n = 3$ , the DARC  $n = 2$  and  $n = 3$  results, providing an uncertainty from 13 – 14% for our recom-

**Table 5.** Effective collision strengths  $\Upsilon_{12}$  and the uncertainty  $\% \Delta$  for Ne II and Ne III ions calculated by the DARC approach using the  $n = 2$  target expansion.

Temperature (K)	Ne II $2s^2 2p^5 (^2P_{3/2}^0) - (^2P_{1/2}^0)$ $\Upsilon_{12}, \% \Delta$	Ne III $2s^2 2p^4 (^3P_2) - (^3P_1)$ $\Upsilon_{12}, \% \Delta$	Ne III $2s^2 2p^4 (^3P_2) - (^3P_0)$ $\Upsilon_{13}, \% \Delta$	Ne III $2s^2 2p^4 (^3P_1) - (^3P_0)$ $\Upsilon_{23}, \% \Delta$
10	0.300, 13.99	0.633, 12.24	0.157, 11.26	0.186, 17.09
40	0.300, 13.74	0.635, 10.76	0.152, 8.50	0.184, 15.83
70	0.300, 13.74	0.636, 10.70	0.151, 8.03	0.183, 15.62
100	0.300, 13.74	0.639, 10.92	0.151, 7.88	0.182, 15.71
150	0.301, 13.82	0.644, 11.45	0.150, 7.63	0.181, 15.65
300	0.301, 13.69	0.640, 12.14	0.150, 7.63	0.177, 16.01
450	0.301, 13.69	0.627, 12.00	0.149, 6.54	0.174, 16.14
600	0.301, 13.57	0.615, 11.15	0.148, 4.46	0.172, 15.63
750	0.302, 13.67	0.604, 9.53	0.148, 2.23	0.169, 13.68
900	0.302, 13.52	0.597, 7.55	0.149, 2.59	0.167, 11.15
1050	0.302, 13.52	0.592, 5.38	0.150, 5.19	0.166, 8.53
1200	0.302, 13.52	0.591, 3.52	0.152, 7.62	0.165, 5.62
1350	0.302, 13.40	0.592, 2.23	0.155, 9.14	0.166, 3.35
1500	0.303, 13.50	0.596, 2.17	0.158, 10.32	0.167, 1.49
1650	0.303, 13.36	0.601, 2.88	0.162, 10.84	0.169, 1.28
1800	0.303, 13.36	0.607, 3.64	0.165, 11.40	0.171, 2.15
1950	0.303, 13.36	0.615, 4.28	0.169, 11.39	0.173, 3.30
2000	0.304, 13.46	0.617, 4.52	0.170, 11.53	0.174, 3.52

mended DARC  $n = 2$  effective collision strengths, as shown in Figure 2.

It is also of interest to consider the differences between the DARC and BP calculations, for the cases when they both have the same configurations. The differences of the effective collision strengths between the DARC  $n = 2$  and BP  $n = 2$  are 11 – 13%, while the DARC  $n = 3$  and BP  $n = 3$  differ by 16 – 18 %.

Considering next  $\text{Ne}^{2+}$ , Figures 3 – 5 present the collision strengths (top) and effective collision strengths (bottom) for three different transitions within the ground term, namely, the  $(^3P_2) - (^3P_1)$  (Fig. 3),  $(^3P_1) - (^3P_0)$  (Fig. 4), and  $(^3P_2) - (^3P_0)$  (Fig. 5) transitions. The collision strengths of different calculations have similar background for each of these transitions. However, the resonance positions are shifted for each calculation, which cause the observed difference in the effective collision strengths. Previous calculations by [McLaughlin et al. \(2011\)](#), which extended down to 2000 K, appears to be consistent with our recommended data, the DARC  $n = 2$  result. The difference between our DARC  $n = 2$  and [McLaughlin et al. \(2011\)](#) are attributed to the fact that that our DARC  $n = 2$  calculation was focused on generating accurate data only for fine structure transitions within the ground term, while [McLaughlin et al. \(2011\)](#) results were focused on higher temperatures and higher n-shells in addition to the levels within the ground term. Again, our recommended collision strength is that produced by the DARC  $n = 2$  calculation, based upon energy level, A-value comparisons with NIST data ([Kramida et al. 2015](#)) and published work, as discussed above.

The uncertainty in the DARC  $n = 2$  results are again provided in a similar fashion using Eq. 3 and the standard deviation of the other BP and DARC models. Values for  $\bar{x}_{best}$  for  $\text{Ne}^{2+}$  are taken from the DARC  $n = 2$ ,  $n = 3$  and BP  $n = 3$  calculations. Considering the effective collision strengths involving the higher excited state transitions (Figs. 4 and 5), the DARC  $n = 2$  model remains our recommended dataset, with uncertainties given by the previously applied method. The uncertainty of the effective collision strengths

from the DARC  $n = 2$  calculations are 2 – 12% (Fig. 3), 1 – 17% (Fig. 4), and 2 – 12% (Fig. 5).

To investigate the sensitivity of the results due to shifting our target energies to NIST values, we consider in Figs. 6 – 8 the effect of these shifts on the collision strengths for the BP  $n = 3$  Ne III calculation. The difference between the two BP calculations (with/without energy shift) is up to 89% for the  $(^3P_2) - (^3P_1)$  transition, up to 39% for the  $(^3P_1) - (^3P_0)$ , and up to 32% for the  $(^3P_2) - (^3P_0)$ . The large difference in the first transition is due to the presence of near threshold resonances. Thus, it is clearly important to include such shifts to NIST in the calculation of accurate low temperature rate coefficients. For this reason all of the data in our recommended dataset, and the data used for the uncertainty estimates, includes such NIST shifts. In general, any system that has near threshold resonances would be particularly sensitive to such shifts, and this should be considered in future calculations of low temperature fine structure rate coefficients.

## 5 SUMMARY

We calculated collision strengths and effective collision strengths for  $\text{Ne}^+$  and  $\text{Ne}^{2+}$  with BP and DARC  $R$ -matrix methods. We are interested in the rates at low temperature (10 – 2000 K), so we focus on small energies (0.007 – 0.107 Ryd. for  $\text{Ne}^+$  and 0.0058 – 0.1658 Ryd. for  $\text{Ne}^{2+}$ ) and perform small scale  $R$ -matrix calculations. After comparing the energies, the Einstein A coefficient ( $A_{ij}$ ), collision strengths ( $\Omega_{ij}$ ) and effective collision strengths ( $\Upsilon_{ij}$ ), we conclude that the DARC  $n = 2$  model provides the most reliable collision strengths and effective collision strengths with the Einstein A coefficients generated by this method being closest to the recommended values (i.e., NIST [Kramida et al. \(2015\)](#)). Further, effective collision strengths computed with the DARC  $n = 2$  approach ([Griffin et al. 2001](#); [McLaughlin et al. 2011](#)) result in rates which agree well with the ex-

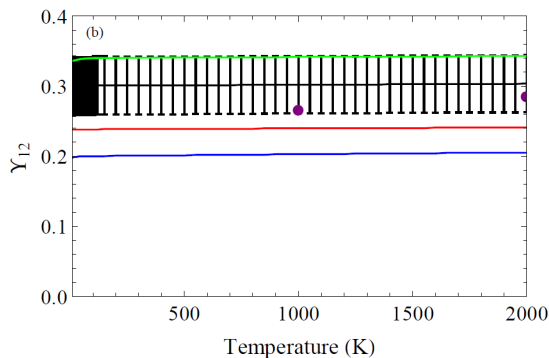
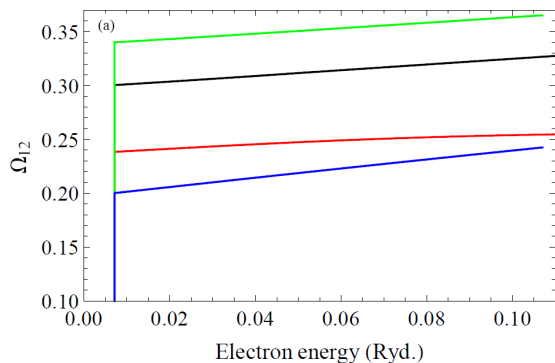


**Figure 2.** Comparison of Ne II collision strengths (a) and effective collision strengths (b) for the  $2s^22p^5 ({}^2P_{3/2}^0) - ({}^2P_{1/2}^0)$  transition between different target expansions: DARC  $n = 2$  (black line), DARC  $n = 3$  (red line), BP  $n = 2$  (green line), and BP  $n = 3$  (blue line). Uncertainty estimates are given for our recommended DARC  $n = 2$  results with comparison to the previous  $R$ -matrix calculation (purple circles) (Griffin et al. 2001).

isting data at higher temperatures calculated by large-scale  $R$ -matrix methods.

## 6 ACKNOWLEDGEMENT

This work was funded under NASA grant NASA-NNX15AE47G. BMMcL would like to thank Professors S. D. Loch, M. S. Pindzola and Auburn University for their hospitality during recent research visits.

## REFERENCES

- Abdel-Naby S. A., Ballance C. P., Lee T.-G., Loch S. D., Pindzola M. S., 2013, *Phys. Rev. A*, **87**, 022708  
 Abdel-Naby S. A., Pindzola M. S., Pearce A. J., Ballance C. P., Loch S. D., 2015, *J. Phys. B: At. Mol. Opt. Phys.*, **48**, 025203  
 Badnell N. R., 1986, *J. Phys. B: At. Mol. Opt. Phys.*, **48**, 025203  
 Berrington K. A., 1987, *J. Phys. B: At. Mol. Phys.*, **20**, 6379

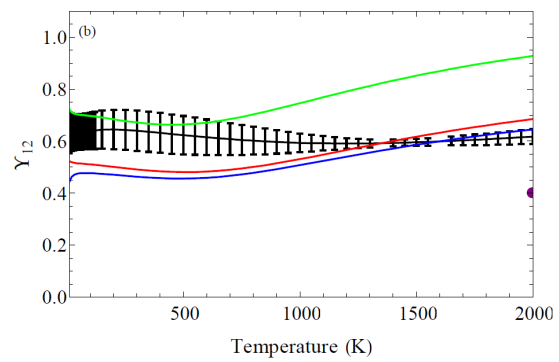
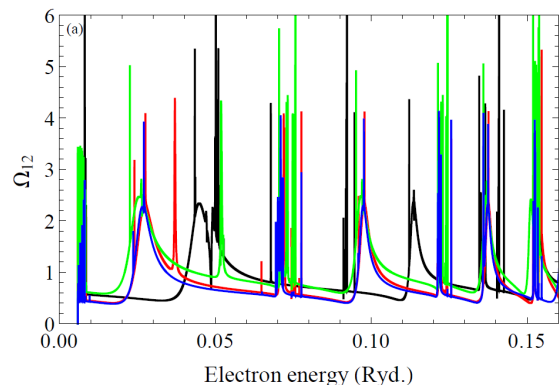


**Figure 3.** Comparison of Ne III collision strengths (a) and effective collision strengths (b) for the  $2s^22p^4 ({}^3P_2) - ({}^3P_1)$  transition between different target expansions: DARC  $n = 2$  (black line), DARC  $n = 3$  (red line), BP  $n = 2$  (green line) and BP  $n = 3$  (blue line). Uncertainty estimates are given for our recommended DARC  $n = 2$  results with comparison to the previous  $R$ -matrix calculation (purple circle) (McLaughlin et al. 2011).

- Berrington K. A., Eissner W., Norrington P. H., 1995, *Comput. Phys. Commun.*, **92**, 290  
 Berrington K. A., Ballance C. P., Griffin D. C., Badnell N. R., 2005, *J. Phys. B: At. Mol. Opt. Phys.*, **38**, 1667  
 Burke P. G., 2011, *R-Matrix Theory of Atomic Collisions: Application to Atomic, Molecular and Optical Processes*. Springer, New York, USA  
 Butler K., Mendoza C., 1984, *Mon. Not. Roy. Astro. Soc.*, **208**, 17P  
 Chang J. J., 1975, *J. Phys. B: At. Mol. Phys.*, **8**, 2327  
 Colgan J., Loch S. D., Pindzola M. S., Ballance C. P., Griffin D. C., 2003, *Phys. Rev. A*, **68**, 032712  
 Dyall K. G., Grant I. P., Johnson C. T., Plummer E. P., 1989, *Comput. Phys. Commun.*, **55**, 425  
 Eissner W., Martins P. d. A. P., Nussbaumer H., Saraph H. E., Seaton M. J., 1969, *Mon. Not. Roy. Astro. Soc.*, **146**, 63  
 Glassgold A. E., Najita J. R., Igea J., 2007, *Astrophys. J.*, **656**, 515  
 Grant I. P., 2007, *Quantum Theory of Atoms and Molecules: Theory and Computation*. Springer, New York, USA  
 Griffin D. C., Badnell N. R. and Pindzola M. S., 1998, *J. Phys. B: At. Mol. Phys.*, **31**, 3713

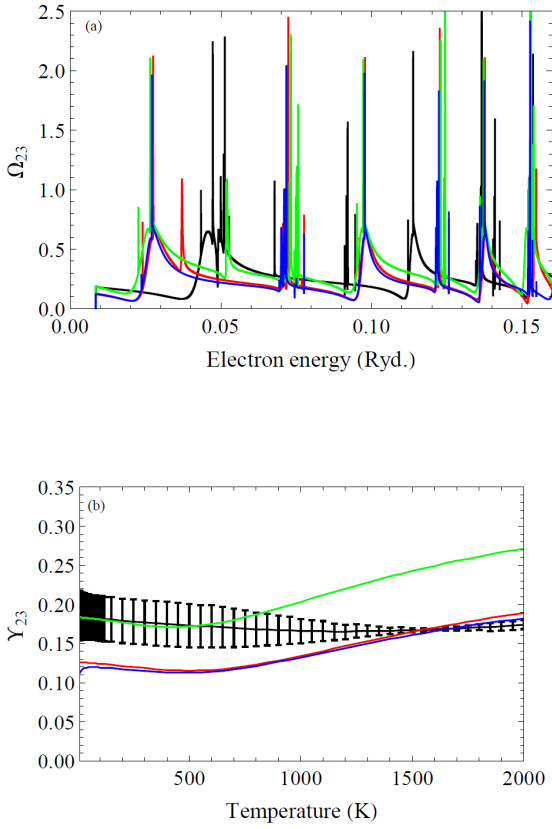


**Figure 4.** Comparison of Ne III collision strengths (a) and effective collision strengths (b) for the  $2s^2 2p^4 (^3P_1) - (^3P_0)$  transition between different target expansions: DARC  $n = 2$  (black line), DARC  $n = 3$  (red line), BP  $n = 2$  (green line) and BP  $n = 3$  (blue line). Uncertainty estimates are given for our recommended DARC  $n = 2$  results.

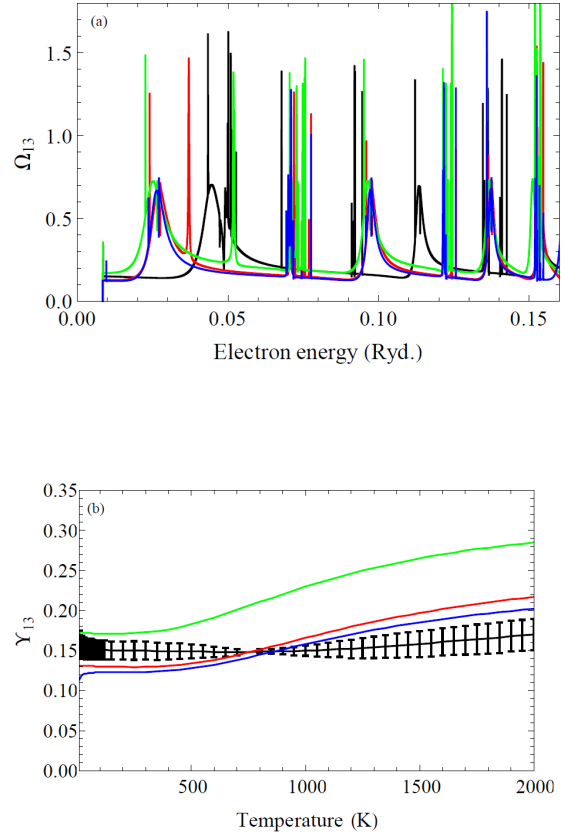


**Figure 5.** Comparison of Ne III collision strengths (a) effective collision strengths (b) for the  $2s^2 2p^4 (^3P_2) - (^3P_0)$  transition between different target expansions: DARC  $n = 2$  (black line), DARC  $n = 3$  (red line), BP  $n = 2$  (green line) and BP  $n = 3$  (blue line). Uncertainty estimates are given for our recommended DARC  $n = 2$  results.

Griffin D. C., Mitnik D. M., Badnell N. R., 2001, *J. Phys. B: At. Mol. Opt. Phys.*, **34**, 4401  
 Johnson C. T., Kingston A. E., 1997, *J. Phys. B: At. Mol. Phys.*, **20**, 2553  
 Kramida A. E., Ralchenko Y., Reader, J. and NIST ASD Team 2015, NIST Atomic Spectra Database (version 5.3), National Institute of Standards, Technology, Gaithersburg, MD, USA, <http://physics.nist.gov/asd>  
 Ludlow J. A., Lee T.-G., Ballance C. P., Loch S. D., Pindzola M. S., 2011, *Phys. Rev. A.*, **84**, 022701  
 Lykins M. L., Ferland G. J., Kisielius R., Chatzikos M., Porter R. L., van Hoof P. A. M., Williams R. J. R. Keenan F. P., Stancil P. C., 2015, *Astrophys. J.*, **807**, 118  
 Malespin C., Ballance C. P., Pindzola M. S., Witthoef M. C., Kallman T. R., Loch S. D., 2011, *Astron. & Astrophys.*, **526**, A115  
 McLaughlin B. M., Bell K. L., 2000, *J. Phys. B: At. Mol. Opt. Phys.*, **33**, 597  
 McLaughlin B. M., Daw A., Bell K. L., 2002, *J. Phys. B: At. Mol. Opt. Phys.*, **35**, 283  
 McLaughlin B. M., Lee T.-G., Ludlow J. A., Landi E., Loch S. D., Pindzola M. S., Ballance C. P., 2011, *J. Phys. B: At. Mol. Opt. Phys.*, **44**, 175206

Meijerink R., Glassgold A. E., Najita J. R., 2008, *Astrophys. J.*, **676**, 518  
 Munoz Burgos J. M., Loch S. D., Ballance C. P., Boivin R. F., 2009, *Astron. & Astrophys.*, **500**, 1253  
 Norrington P. H., Grant I. P., 1981, *J. Phys. B: At. Mol. Phys.*, **14**, L261  
 Pradhan A. K., 1974, *J. Phys. B: At. Mol. Phys.*, **7**, L503  
 Saraph H. E., 1978, *Comput. Phys. Commun.*, **15**, 247  
 Saraph H. E., Tully J. A., 1994, *Astron. Astrophys. Suppl.*, **107**, 29  
 Schöier F. L., van der Tak F. F. S., van Dishoeck E. F., Black J. H., 2005, *Astron. Astrophys.*, **432**, 369  
 Seaton M. J., 1953, *Proc. Roy. Soc. A*, **218**, 400  
 Witthoef M. C., Whiteford A. D., Badnell N. R., 2007, *J. Phys. B: At. Mol. Opt. Phys.*, **40**, 2969  
 Wu D., Loch S. D., Pindzola M. S., Ballance C. P., 2012, *Phys. Rev. A.*, **85**, 012711

This paper has been typeset from a  $\text{\TeX}/\text{\LaTeX}$  file prepared by the author.



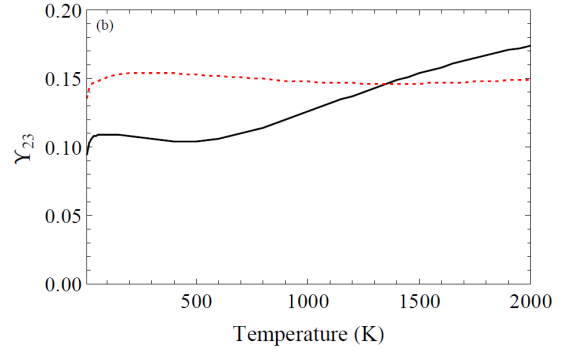
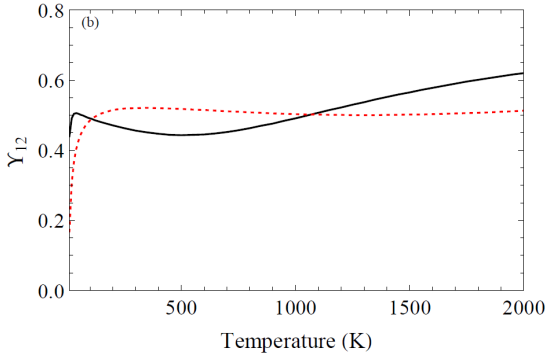
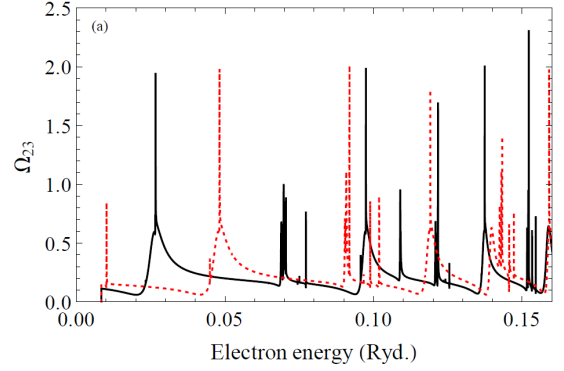
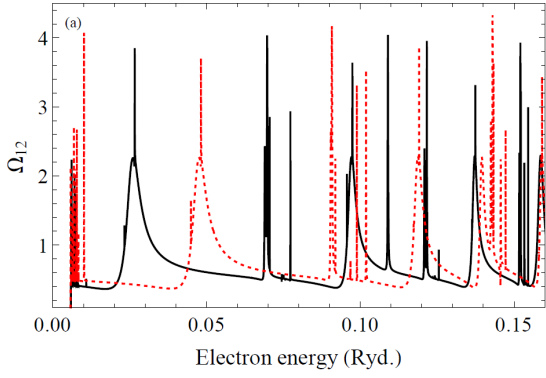


**Figure 6.** Comparison of Ne III collision strengths (a) and effective collision strengths (b) for the  $2s^2 2p^4$  ( $^3P_2$ ) - ( $^3P_1$ ) transition: BP  $n = 3$  with (black solid line) and without (red dotted line) the energy shift.

**Figure 7.** Comparison of the Ne III collision strengths (a) and effective collision strengths (b) for the  $2s^2 2p^4$  ( $^3P_1$ ) - ( $^3P_0$ ) transition: BP  $n = 3$  with (black solid line) and without (red dotted line) the energy shift.

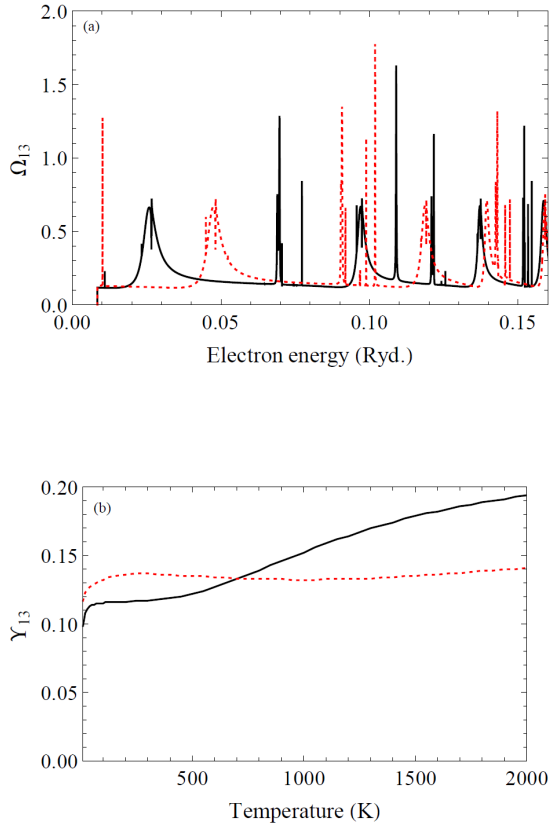


**Figure 8.** Comparison of Ne III collision strengths (a) and effective collision strengths (b) for the  $2s^2 2p^4 (^3P_2) - (^3P_0)$  transition: BP  $n = 3$  with (black solid line) and without (red dotted line) the energy shift.